J|A|C|S
ARTICLES
Published on Web 05/01/2007

Stabilized Phosphatidylinositol-5-Phosphate Analogues as Ligands for the Nuclear Protein ING2: Chemistry, Biology, and Molecular Modeling

Wei Huang,[†] Honglu Zhang,[†] Foteini Davrazou,[‡] Tatiana G. Kutateladze,[‡] Xiaobing Shi,[§] Or Gozani,[§] and Glenn D. Prestwich*[,†]

Contribution from the Department of Medicinal Chemistry, The University of Utah, 419 Wakara Way, Suite 205, Salt Lake City, Utah 84108-1257, Department of Pharmacology, University of Colorado Health Sciences Center, Aurora, Colorado 80045-0511, and Department of Biological Sciences, Stanford University, Palo Alto, California 94305

Received January 10, 2007; E-mail: gprestwich@pharm.utah.edu

Abstract: The interaction of PtdIns(5)P with the tumor suppressor protein ING2 has been implicated in the regulation of chromatin modification. To enhance the stability of PtdIns(5)P for studies of the biological role in vivo, two phosphatase-resistant moieties were used to replace the labile 5-phosphate. The total asymmetric synthesis of the 5-methylenephosphonate (MP) and 5-phosphothionate (PT) analogues of PtdIns(5)P is described herein, and the resulting metabolically stabilized lipid analogues were evaluated in three ways. First, liposomes containing either the dioleoyl MP or PT analogues bound to recombinant ING2 similar to liposomes containing dipalmitoyl PtdIns(5)P, indicating that the replacement of the hydrolyzable 5-phosphate group does not compromise the binding. Second, the dioleoyl MP and PT PtdIns(5)P analogues were equivalent to dipalmitoyl PtdIns(5)P in augmenting cell death induced by a DNA double-strand break in HT1080 cells. Finally, molecular modeling and docking of the MP or PT analogues to the C-terminus PtdInsP-binding region of ING2 (consisting of a PHD finger and a polybasic region) revealed a number of complementary surface and electrostatic contacts between the lipids and ING2.

Introduction

Phosphoinositide ($PtdInsP_n$) signaling involves a wide variety proteins that exhibit lipid recognition, kinase, phosphatase, or phospholipase activities.[1,2] One relatively rare phosphoinositide, PtdIns(5)P, has been implicated as a critical regulator of nuclear signaling events in cell-cycle progression,[3] for DNA damage-dependent ING2 association with chromatin,[4] and to inhibit ATX1 gene expression programs.[5] Still, relatively few details are understood with respect to the signaling functions of PtdIns-(5)P due to the paucity of well-characterized nuclear PtdIns-(5)P binding domains. The interaction discovered between PtdIns(5)P and ING2 (inhibitor of growth protein 2) was shown to require both a C-terminus plant homeodomain (PHD) zinc finger motif and a short stretch of polybasic residues[6] and implicated ING2 as a potential nuclear target for PtdIns(5)P.

The ING family of proteins is highly conserved from yeast to humans,[7] and different members are native subunits of histone acetyl transferase (HAT) and histone deacetylase (HDAC) complexes.[8] Mammalian ING proteins are candidate tumor suppressor proteins, which cooperate with p53 to induce cellular growth arrest and apoptosis; for example, overexpression of ING2 stimulates acetylation of p53.[9,10] As a result, the ING family is alleged to link chromatin regulation with p53 function and tumor suppression. ING2 contains a PHD finger that recognizes trimethylated at lysine 4 histone H3 tail.[11,12] The ING2 PHD finger is also required for the interaction with PtdIns(5)P,[6] and together with the 18-residue polybasic region C-terminal to the PHD domain, is necessary and sufficient for phosphoinositide binding by ING2.[13] Thus, a model of ING2 with both of PHD domain and polybasic region is required to understand the binding and physiological activities of PtdIns(5)P.

[†] The University of Utah.
[‡] University of Colorado Health Sciences Center.
[§] Stanford University.

(1) Payrastre, B.; Missy, K.; Giuriato, S.; Bodin, S.; Plantavid, M.; Gratacap, M. *Cell. Signalling* **2001**, *13*, 377−387.
(2) Prestwich, G. D. *Chem. Biol.* **2004**, *11*, 619−637.
(3) Clarke, J. H.; Letcher, A. J.; D'Santos, C. S.; Halstead, J. R.; Irvine, R. F.; Divecha, N. *Biochem. J.* **2001**, *357*, 905−910.
(4) Jones, D. R.; Divecha, N. *Curr. Opin. Genet. Dev.* **2004**, *14*, 196−202.
(5) Alvarez-Venegas, R.; Sadder, M.; Hlavacka, A.; Baluska, F.; Xia, Y.; Lu, G.; Firsov, A.; Sarath, G.; Moriyama, H.; Dubrovsky, J.; Avramova, Z. *Proc. Natl. Acad. Sci. U.S.A.* **2006**, *103*, 6049−6054.
(6) Gozani, O.; Karuman, P.; Jones, D. R.; Ivanov, D.; Cha, J.; Lugovskoy, A. A.; Baird, C. L.; Zhu, H.; Field, S. J.; Lessnick, S. L.; Villasenor, J.; Mehrotra, B.; Chen, J.; Rao, V. R.; Brugge, J. S.; Ferguson, C. G.; Payrastre, B.; Myszka, D. G.; Cantley, L. C.; Wagner, G.; Divecha, N.; Prestwich, G. D.; Yuan, J. *Cell* **2003**, *114*, 99−111.
(7) Brunecky, R.; Lee, S.; Rzepecki, P. W.; Overduin, M.; Prestwich, G. D.; Kutateladze, A. G.; Kutateladze, T. G. *Biochemistry* **2005**, *44*, 16064−16071.
(8) Feng, X.; Hara, Y.; Riabowol, K. *Trends Cell Biol.* **2002**, *12*, 532−538.
(9) Garkavtsev, I.; Grigorian, I. A.; Ossovskaya, V. S.; Chernov, M. V.; Chumakov, P. M.; Gudkov, A. V. *Nature* **1998**, *391*, 295−298.
(10) Nagashima, M.; Shiseki, M.; Miura, K.; Hagiwara, K.; Linke, S. P.; Pedeux, R.; Wang, X. W.; Yokota, J.; Riabowol, K.; Harris, C. C. *Proc. Natl. Acad. Sci. U.S.A.* **2001**, *98*, 9671−9676.
(11) Shi, X.; Gozani, O. *J. Cell. Biochem.* **2005**, *96*, 1127−1136.
(12) Pena, P. V.; Davrazou, F.; Shi, X.; Walter, K. L.; Verkhusha, V. V.; Gozani, O.; Zhao, R.; Kutateladze, T. G. *Nature* **2006**, *442*, 100−103.
(13) Kaadige, M. R.; Ayer, K. E. *J. Biol. Chem.* **2006**, *281*, 28831−28836.

 10.1021/ja070195b CCC: $37.00 **© 2007 American Chemical Society**

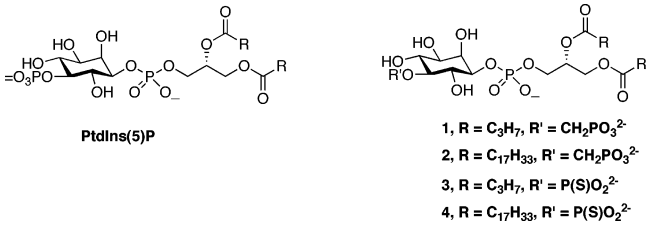

Figure 1. 5-Methylenephosphonate and 5-phosphothionate analogues of PtdIns(5)P.

Although the crystal structure of the ING2 PHD domain has been determined[12] and several homologous structures of ING proteins are available through the PDB bank, at present no 3D structure of ING2 that includes the flexible C-terminal polybasic region is available. Thus, further characterization of the structure and function of the ING2-C-terminus will benefit from the use of modified PtdIns(5)P ligands.

In vivo studies of PtdIns(5)P are problematic because of its rapid metabolism. Specifically, three important metabolic pathways are presently known to utilize PtdIns(5)P as a substrate. Two pathways involve kinases; PtdIns(4,5)P_2 is produced by the action of PtdIns(5)P 4-kinase, and PtdIns(3,5)P_2 can be produced by PtdIns 3-kinase.[2,14,15] The third route involves a ubiquitous cellular phosphatase activity that metabolizes PtdIns(5)P to PtdIns.

We have recently pursued a program to prepare metabolically stabilized, e.g., phopholipase- and phosphatase-resistant analogues of the phosphoinositides PtdIns(3)P,[16,17] PtdIns(4,5)P_2,[18] and PtdIns(3,4,5)P_3.[19] In these examples, as with analogues the phosphatase-labile lysophosphatidic acid (LPA),[20] methyl phosphonates, fluoromethyl phosphosphonates, phosphorothionates, and methylenephosphonates were used to replace the natural phosphomonoester or phosphodiester moieties. Herein we describe the total asymmetric synthesis of the 5-methylenephosphonate (MP) and 5-phosphothionate (PT) analogues of PtdIns(5)P (Figure 1) as water-soluble ligands with short dibutanoyl chains or as lipid-soluble amphiphiles with dioleoyl chains. We show that PtdIns(5)P analogues interact with the C-terminal region of ING2 using liposome binding assays. Further, cellular studies demonstrate that the MP and PT analogues are as bioactive as PtdIns(5)P in augmenting cell death induced by DNA damage. Finally, we construct 3D models of the ING2 polybasic region using homology modeling algorithms and computationally dock the PtdIns(5)P analogues to these models.

Results and Discussion

Chemical Synthesis of Stabilized Phosphatidylinositol-5-Phosphate Analogues. The syntheses of the metabolically stabilized PtdIns(5)P analogues were based on modifications of routes to the corresponding PtdIns(3)P analogues.[16,17] Each contained the following strategic steps: (a) selective protection of positions of inositol,[21] in particular using the TBDPS group for the 1-position, benzoate group for 5-position, and MOM group for 2,3,4,6-positions; (b) introduction of the MP or PT functionality in protected form at the 5-position; (c) introduction of the diacylglycerol phosphate at the 1-position using phosphoramidite chemistry.

Scheme 1 illustrates the preparation of the 5-MP-PtdIns(5)P analogue. D-Camphor dimethyl acetal[22] gave exclusively the 2,3-bornanediyl-*myo*-inositol,[23] which was then regioselectively silylated at 1-OH with TBDPSCl.[24] After reaction with benzoyl chloride and removal of bornanediyl group, the 5-benzoyl-1-TBDPS intermediate was isolated from the mixture containing 4-benzoate and 4,5-bisbenzoate products. All the remaining hydroxyl groups were protected as methoxymethyl (MOM) ethers to give intermediate **6**.[21] After removal of benzoate group with sodium methoxide, key intermediate **7** was obtained from *myo*-inositol in six steps.

Dimethyl phosphonomethyltriflate, which is required for installation of methylenephosphonate to the 5-position of **7**, was prepared as described.[25,26] The alkylation of **7** with dimethyl phosphonomethyltriflate was employed using NaH/THF in 86% yield. Use of *n*-BuLi[17,27] as the base in this reaction resulted in more byproducts and a lower yield. Then, the TBDPS group of **8** was removed with tetrabutylammonium fluoride trihydrate (TBAF·3H_2O) at room temperature for 4 h to give alcohol **9**. Separately, the two diacylglyceryl phosphoramidites **10a** and **10b** were prepared from 1,2-*O*-isopropylidene-*sn*-glycerol in five steps as reported.[17,28] Then, in the presence of 1*H*-tetrazole, **9** was treated with **10a** (or **10b**), followed by oxidation with *t*-BuOOH to give the fully protected intermediate **11a** (or **11b**). The cyanoethyl (CE) group was removed in the presence of triethylamine (TEA) and bis(trimethylsilyl)trifluoroacetamide (BSTFA),[29] and the phosphate methyl ester and MOM ether were removed using TMSBr and BSTFA.[21] After complete evaporation of organic solvent in vacuo, the crude product was treated with Dowex ion-exchange resin[17] to yield the 5-MP analogues of PtdIns(5)P (**1** and **2**, Scheme 1).

To obtain the 5-PT analogues of PtdIns(5)P, we first attempted to use the protected 5-phosphorothioate intermediate **13**, prepared by phosphitylation of alcohol **7** with bis(2-cyanoethyl)diisopropylphosphorodiamidite followed by oxidation with sulfur in CS_2/pyridine. The removal of TBDPS group of obtained product **12** was achieved by using HF−pyridine complex (Scheme 2) instead of TBAF because the cyanoethyl group was labile to cleavage by TBAF.[17] However, the long reaction time (3 weeks) proved to be a significant disadvantage of this method. We thus abandoned this intermediate and solved the problem by replacing the TBDPS group with the triethylsilyl (TES) group[19] as illustrated in Scheme 3.

(14) Whiteford, C. C.; Brearley, C. A.; Ulug, E. T. *Biochem. J.* **1997**, *323* (Part 3), 597−601.
(15) Peng, J.; Prestwich, G. D. *Tetrahedron Lett.* **1998**, *39*, 3965−3968.
(16) Xu, Y.; Lee, S. A.; Kutateladze, T. G.; Sbrissa, D.; Shisheva, A.; Prestwich, G. D. *J. Am. Chem. Soc.* **2006**, *128*, 885−897.
(17) Gajewiak, J.; Xu, Y.; Lee, S. A.; Kutateladze, T. G.; Prestwich, G. D. *Org. Lett.* **2006**, *8*, 2811−2813.
(18) Zhang, H.; Xu, Y.; Zhang, Z.; Liman, E. R.; Prestwich, G. D. *J. Am. Chem. Soc.* **2006**, *128*, 5642−5643.
(19) Zhang, H.; Markadieu, N.; Beawens, R.; Erneux, C.; Prestwich, G. D. *J. Am. Chem. Soc.* **2006**, *128*, 16464−16465.
(20) Prestwich, G. D.; Xu, Y.; Qian, L.; Gajewiak, J.; Jiang, G. *Biochem. Soc. Trans.* **2005**, *33*, 1357−1361.
(21) Kubiak, R. J.; Bruzik, K. S. *J. Org. Chem.* **2003**, *68*, 960−968.
(22) Lindberg, J.; Ohberg, L.; Garegg, P. J.; Konradsson, P. *Tetrahedron* **2002**, *58*, 1387−1398.
(23) Pietrusiewicz, K. M.; Salamonczyk, G. M.; Bruzik, K. S. *Tetrahedron* **1992**, *48*, 5523−5542.
(24) Bruzik, K. S.; Tsai, M. *J. Am. Chem. Soc.* **1992**, *114*, 6361−6374.
(25) Jeanmaire, T.; Hervaud, Y.; Boutevin, B. *Phosphorus, Sulfur Silicon Relat. Elem.* **2002**, *177*, 1137−1145.
(26) Xu, Y.; Flavin, M. T.; Xu, Z. Q. *J. Org. Chem.* **1996**, *61*, 7697−7701.
(27) Kulagowski, J. J.; Baker, R.; Fletcher, S. R. *J. Chem. Soc., Chem. Commun.* **1991**, 1649−1650.
(28) Chen, J.; Profit, A. A.; Prestwich, G. D. *J. Org. Chem.* **1996**, *61*, 6305−6312.
(29) Heeb, N. V.; Nambiar, K. P. *Tetrahedron Lett.* **1993**, *34*, 6193−6196.

Scheme 1. Synthesis of 5-Methylenephosphonate Analogues of PtdIns(5)P[a]

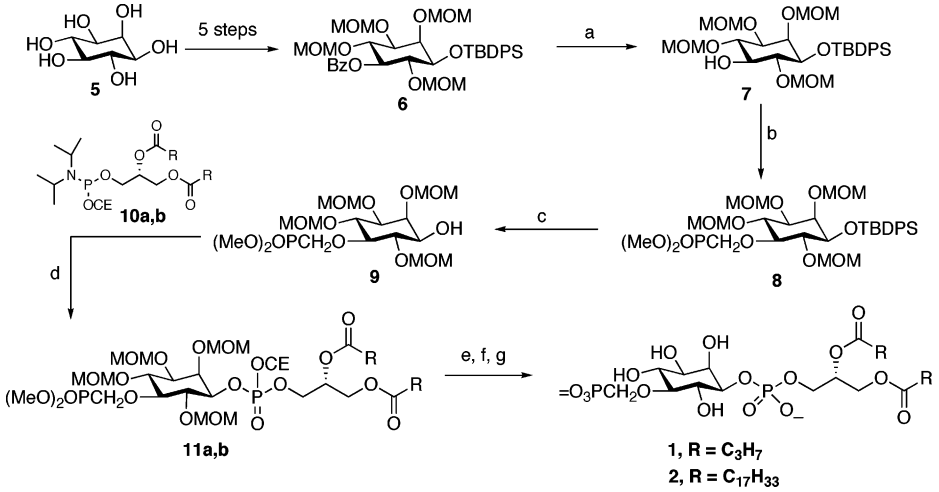

[a] Reagents and conditions: (a) NaOMe, MeOH, room temperature, 24 h; (b) dimethyl phosphonomethyltriflate, NaH, THF, 0 °C, then room temperature, 12 h; (c) TBAF·3H_2O, THF, room temperature, 4 h; (d) 1*H*-tetrazole, CH_2Cl_2, Ar, room temperature, 24 h, then *t*-BuOOH, 1 h; (e) TEA, BSTFA, MeCN, Ar, room temperature, 24 h; (f) TMSBr, BSTFA, Ar, room temperature, 10 h; (g) MeOH, room temperature, 1 h.

Scheme 2. Synthesis of Intermediate **13**[a]

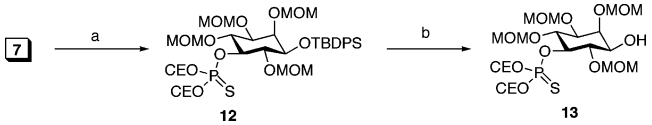

[a] Reagents and conditions: (a) bis(2-cyanoethyl)diisopropylphosphorodiamidite, 1*H*-tetrazole, MeCN, Ar, room temperature, 2 h, then sulfur, CS_2/Py (1:1), room temperature, 3 h; (b) HF−Py, THF, room temperature, 3 weeks.

Scheme 3 shows the preparation of the 5-PT analogues PtdIns(5)P. Thus, 5-benzoyl-1-TBDPS-2,3,4,6-tetrakis(MOM)-inositol (**6**) was treated with TBAF to remove the 1-TBDPS ether; this was then replaced with TES ether by using TESCl. Although two additional steps were required, this change of protecting groups improves overall yield and reduces side products as found for a 3-PT analogue of PtdIns(3,4,5)P_3.[19] After debenzoylation of **14** with diisobutyl aluminum hydride (DIBAL-H), the phosphorothioate group was introduced in the 5-position as shown in Scheme 2. Deprotection of the TES group of **16** with NH_4F gave intermediate **13** efficiently and in high yield. Then, the diacylglycerophosphodiester linkage to the 1-position of **13** was created using either **10a** (or **10b**) and 1*H*-tetrazole followed by oxidation. After deprotection of cyanoethyl group and MOM group, the final products of 5-PT analogues of PtdIns(5)P (**3** and **4**) were obtained.

Liposome Binding Assay. To determine the effect of the PtdIns(5)P head group modifications on the inositol ring recognition by ING2, PtdIns(5)P analogues were evaluated using liposome binding assays (Figure 2). The C-terminal region of ING2 (amino acids 200−280 of ING2) has been shown to interact with PtdIns(5)P in vitro and in vivo.[6] In the absence of any phosphoinositide in the liposome composition or in the presence of unphosphorylated PtdIns, the GST-fused C-terminal region of ING2 (GST−ING2) remains primarily soluble. With the parent ligand dipalmitoyl PtdIns(5)P embedded in the liposome, GST−ING2 was strongly associated with the liposome fraction. Both modified lipids, 5-MP-PtdIns(5)P (**2**) and 5-PT PtdIns(5)P (**4**), bound GST−ING2 with nearly the same efficiency as the unmodified lipid, suggesting that these synthetic analogues could substitute for PtdIns(5)P in biochemical and biological assays.

HT1080 Cell Death Assay. ING2 overexpression triggers a number of molecular events including p53 acetylation that can culminate in the induction of apoptosis;[10] the lipid binding activity of ING2 is critical for these activities.[6] Furthermore, endogenous generation of nuclear PtdIns(5)P is involved in cellular responses to genotoxic stress, through regulation of ING2 and likely a number of additional factors.[30] To test whether the 5-PT and 5-MP analogues of PtdIns(5)P would retain the same function in this pathway, we measured the HT1080 cell death response to DNA damage following treatment with dipalmitoyl PtdIns(5)P and/or with 5-MP-PtdIns(5)P (**2**) and 5-PT PtdIns(5)P (**4**) (Figure 3). PtdIns(5)P shows a statistically significant, albeit small, enhancement in the level of cell death induced by neocarzinostatin (NCS) treatment alone in HT1080 cells. Both the 5-MP-PtdIns(5)P analogue **2** and 5-PT PtdIns(5)P analogue **4** show an equivalent effect in promoting cell death. These results demonstrate a biological effect of the metabolically stabilized PtdIns(5)P analogues in this nuclear stress response pathway.

Molecular Modeling. Combining known biochemical, structural, and functional data on the ING2 PHD domain and polybasic region activities, we sought to model the C-terminal tail of ING2 to gain insights into its interactions with PtdIns(5)P analogues. However, little is known concerning the 3D structure of the last 18 residues, which is likely to be a random coil. To further characterize the structure of this region, we built 20 homology models of the ING2 C-terminus (residues 202−281) by employing MODELLER,[31−33] a set of algorithms for homology modeling. Each computed model contained the conserved PHD domain and different polybasic regions based on reported crystal structures. These models included multiple possible stereochemical geometries for the polybasic tail as anticipated for simulation of a random coil. Next, we employed

(30) Jones, D.; Bultsma, Y.; Kuene, W.-J.; Halstead, J.; Elouarrat, D.; Mohammed, S.; Heck, A.; D'Santos, C.; Divecha, N. *Mol. Cell* **2006**, *23*, 685−695.
(31) Sali, A.; Blundell, T. L. *J. Mol. Biol.* **1993**, *234*, 779−815.
(32) Marti-Renom, M. A.; Stuart, A.; Fiser, A.; Sanchez, R.; Melo, F.; Sali, A. *Annu. Rev. Biophys. Biomol. Struct.* **2000**, *29*, 291−325.
(33) Fiser, A.; Do, R. K.; Sali, A. *Protein Sci.* **2000**, *9*, 1753−1773.

Scheme 3. Synthesis of 5-Phosphothionate Analogues of PtdIns(5)P[a]

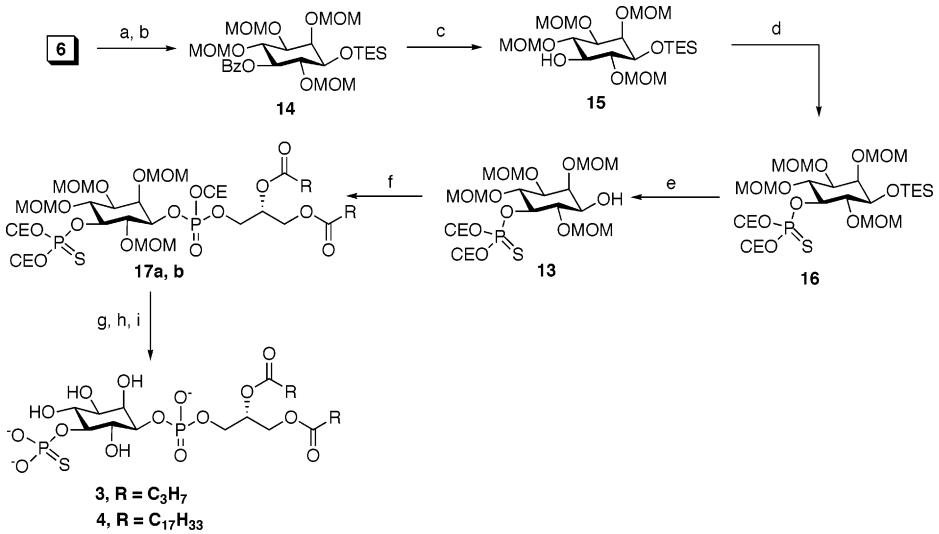

[a] Reagents and conditions: (a) TBAF·3H_2O, DMF, room temperature, 6 h; (b) triethylsilyl chloride, imidazole, CH_2Cl_2, room temperature, 15 h; (c) DIBAL-H, CH_2Cl_2, −78 °C, 2 h; (d) bis(2-cyanoethyl)diisopropylphosphorodiamidite, 1*H*-tetrazole, MeCN, Ar, room temperature, 2 h, then sulfur, CS_2/Py (1:1), room temperature, 6 h; (e) NH_4F, MeOH, room temperature, 20 h; (f) **10a** (or **10b**), 1*H*-tetrazole, CH_2Cl_2, Ar, room temperature, 24 h, then *t*-BuOOH, 1 h; (g) TEA, BSTFA, MeCN, Ar, room temperature, 24 h; (h) TMSBr, BSTFA, Ar, room temperature, 2 h; (i) MeOH, room temperature, 1 h.

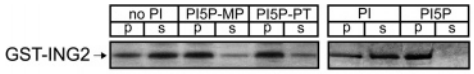

Figure 2. PtdIns(5)P analogues are efficiently recognized by ING2. The SDS−PAGE gels show the partitioning of the GST-fused C-terminal tail of ING2 between the supernatant fraction (S) and the liposome pellet (P). To better mimic native membranes, liposomes were prepared from phospholipids typically found in bilayers including PtdCho, PtdEtn, PtdSer in a ratio of 65:26:9 or PtdCho, PtdEtn, PtdSer and the corresponding phosphoinositide in a ratio of 54:22:9:15.

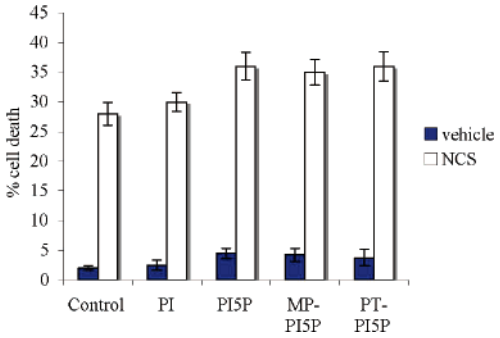

Figure 3. PtdIns(5)P and analogues augment cell death induced by neocarzinostatin (NCS) treatment. Cell death was measured in HT1080 cells treated with 10 μM of the indicated lipid or no lipid control, ± 45 nM NCS. The error bars represent the mean ± SEM for four experiments.

AutoDock 3.0.5[34−36] to dock the ligands to ING2 models successively and performed LIGPLOT 4.4.2[37] into study the preferred binding conformation and association within the ING2−PtdIns(5)P complex.

The sequence of human ING2[38] (202−281) was provided as input data, and five template structures were generated with good sequence identities by SWISS-MODEL server (Figure 4A).[39−41] They are solution structures of ING family proteins in the PDB bank (http://www.rcsb.org/);[42] 1wes, 1weu, and 1wen are PHD domains of ING1-like protein; 2q6g is PHD domain of ING2; 1x4i is C-terminal of ING3 which contains 20 models extending beyond the PHD domain, and these models provide the diverse templates for the C-terminal tail. After sequence alignment by MODELLER, the automodel mode of MODELLER was used, based on each 1x4i model and the other templates, thus affording 20 primary ING2 structures. Then, after side-chain modeling and energy minimization for each structure an ensemble of the 20 homology models of the ING2 C-terminus was obtained. As shown in Figure 4, parts B and C, these models contain a highly conserved PHD domain which ends with a short helix (normally from Pro257 to Lys265), followed by a highly divergent set of orientations for the remainder of the polybasic region.

The polybasic region contains three arginine and five lysine residues that can form a binding pocket for the phosphoinositide. First, we studied the 3D structure of each model and observed the key features of each one. The helix C-terminal from the PHD domain (Pro257 to Lys265) showed good identity for the majority of models, and the side chain of Lys265 was close to the region of Tyr255 and Lys253 within the PHD domain (Figure 5, parts A and B). However, the polybasic tails were widely divergent in the absence of a phosphoinositide ligand. For example, in model 1 (Figure 5A), the end residues (Arg281, Arg279, Arg278) move to 25 Å away from the PHD domain (Arg278 to Lys253), such that the Arg and Lys residues in the polybasic tail could not form an effective pocket. In contrast, in model 2 (Figure 5B), the tail loops back toward the PHD domain (Tyr255, Lys253) with proper torsion angles (9 Å from Arg278 to Lys253), forming a more reasonable binding pocket.

(34) Goodsell, D. S.; Olson, A. J. *Proteins* **1990**, *8*, 195−202.
(35) Morris, G. M.; Goodsell, D. S.; Huey, R.; Olson, A. J. *J. Comput.-Aided Mol. Des.* **1996**, *10*, 293−304.
(36) Morris, G. M.; Goodsell, D. S.; Halliday, R. S.; Huey, R.; Hart W. E.; Belew, R. K.; Olson, A. J. *J. Comput. Chem.* **1998**, *19*, 1639−1662.
(37) Wallace, A. C.; Laskowski, R. A.; Thornton, J. M. *Protein Eng.* **1995**, *8*, 127−134.
(38) Wagner, M. J.; Gogela-Spehar, M.; Skirrow, R. C.; Johnston, R. N.; Riabowol, K.; Helbing, C. C. *J. Biol. Chem.* **2001**, *276*, 47013−47020.
(39) Schwede, T.; Kopp, J.; Guex, N.; Peitsch, M. C. *Nucleic Acids Res.* **2003**, *31*, 3381−3385.
(40) Kopp, J.; Schwede, T. *Nucleic Acids Res.* **2004**, *32*, D230−D234.
(41) Guex, N.; Peitsch, M. C. *Electrophoresis* **1997**, *18*, 2714−2723.
(42) Westbrook, J.; Feng, Z.; Chen, L.; Yang, H.; Berman, H. M. *Nucleic Acids Res.* **2003**, *31*, 489−491.

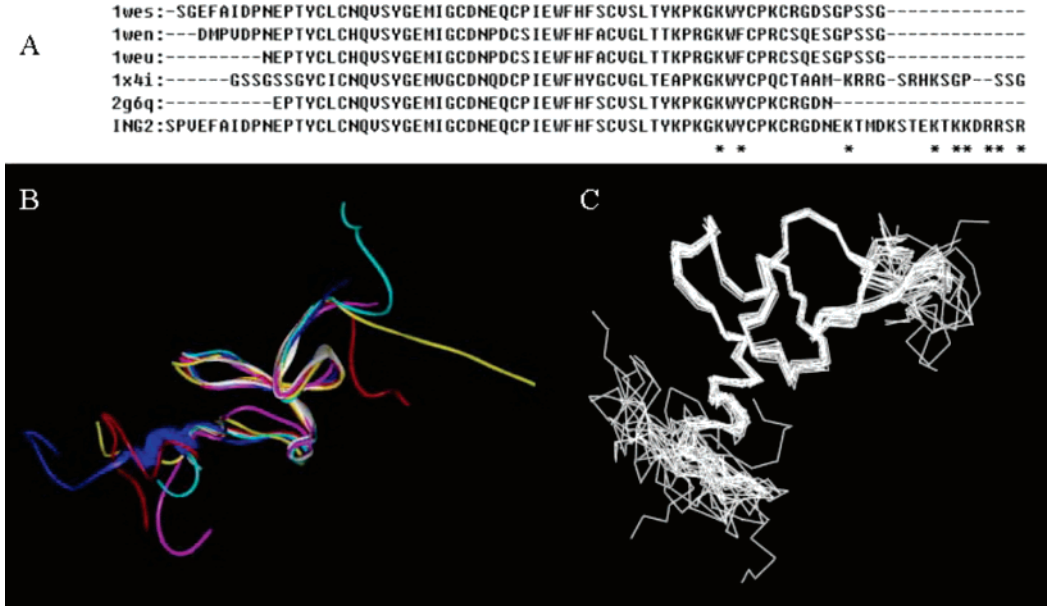

Figure 4. (A) Sequence alignment of ING2 (202−281) with related family members from PDB. The alignment was performed under the module of ALIGNMENT in MODELLER. (B) Structural alignment of the ING2 model (one of 20 models, red), 2g6q (white), 1x4i (blue), 1weu (purple), 1wes (cyan), and 1wen (yellow). PHD domains are the conserved fractions in the center of the structures, end with a short helix, and the following tails on the left side are polybasic regions. (C) Twenty ING2 models built by MODELLER. The multiorientation coils on the left side are polybasic C-termini.

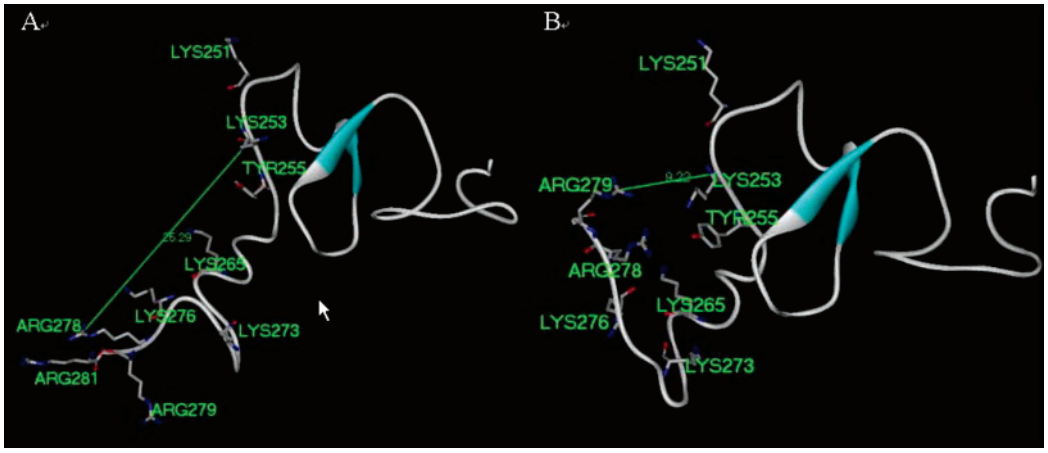

Figure 5. Structural analysis of two representative models from 20 models generated by homology modeling: (A) model 1; (B) model 2.

Indeed, Arg279, Arg278, and Lys276 form a proper site with Lys265 and the PHD domain contributing to the pocket. In this case, Lys265 is located in the site center and serves as a "bridge" to connect the PHD domain and polybasic tail. Among the 20 models, six contained a pocket similar to that of model 2. The other 14 models had extended tails (as in model 1) but with widely divergent orientations.

Furthermore, we docked diC_4-PtdIns(5)P to each of the 20 models using AutoDock3.0.5. The models containing a reasonable binding pocket that included the polybasic tail, helix, and PHD domains provided better binding scores than other models. Supporting Information Figure S1A−S1D presents the binding modes of diC_4-PtdIns(5)P with models 2, 7, 9, and 10 which give the highest scores and most reasonable conformations. These models all gave similar binding modes with diC_4-PtdIns(5)P. The inositol ring was located in the area of Arg279, Arg278, Asp277, and Lys265, and the phosphate and hydroxyl groups formed good hydrogen bond networks with these residues. The diacyl groups of lipid approached Tyr255 and Lys253 of the PHD domain.

Finally, after overall examination on binding energy and structure rationality of these four models, we selected model 2 as the ING2 C-terminal model to compare the binding features of di$C_{18:1}$-PtdIns(5)P with the corresponding metabolically stabilized analogues. The binding conformations of di$C_{18:1}$-PtdIns(5)P, 5-MP-di$C_{18:1}$-PtdIns(5)P (**2**), and 5-PT-di$C_{18:1}$-PtdIns(5)P (**4**) are shown in Figure 6. These three compounds have similar conformations. The inositol ring is located in the pocket, and one of acyl groups is oriented toward the PHD domain (Tyr255, Lys253) and the other orients to another part of polybasic tail (Arg260, Lys273). The 5-phosphate of the inositol head group is located proximal to Arg278, while the 1-phosphodiester linkage is proximal to Arg279 (Figure 6). These results indicated a good steric simulation of chemical geometry. We employed LIGPLOT4.4.2 to test the hydrogen bonds and hydrophobic contacts between ligands and ING2. Supporting Information Figures S2−S4 show that the hydrogen bonds for the MP and PT analogues are almost identical with those for di$C_{18:1}$-PtdIns(5)P. However, there are more hydrophobic contacts observed for the longer acyl chains, thus

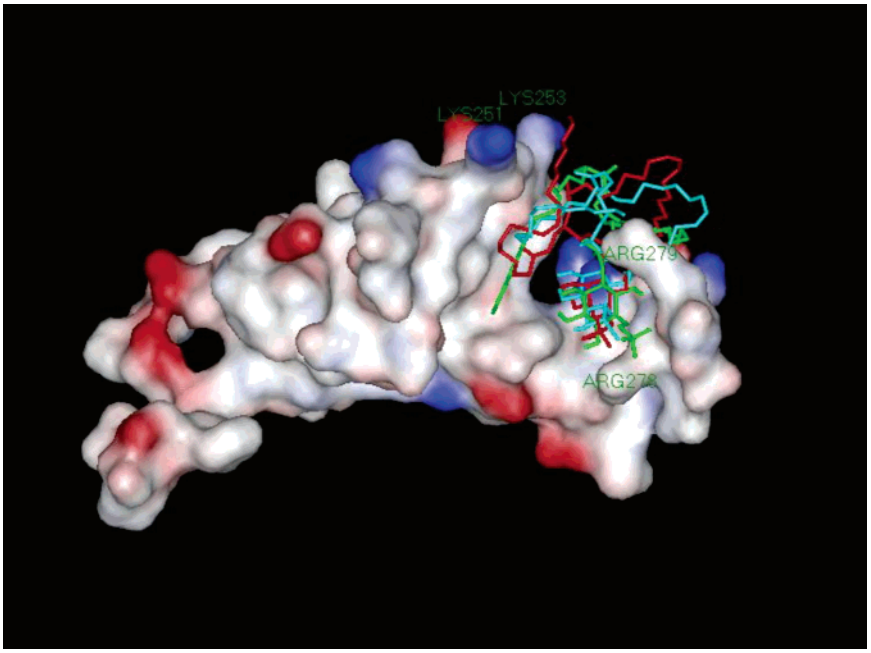

Figure 6. Docking conformations of di$C_{18:1}$-PtdIns(5)P (red), di$C_{18:1}$-MP-PtdIns(5)P (**2**, green), and di$C_{18:1}$-PT-PtdIns(5)P (**4**, cyan) in the surface of the ING2 C-terminal model.

enhancing interactions with the PHD domain. This can rationalize our observations (unpublished results) that the dioleoyl analogues showed higher affinity than the dibutanoyl analogues in each of the binding assay formats tested.

Finally, in agreement with the modeling studies, Lys 251, Lys 253, W254, and G261 residues of the PHD finger and the polybasic region of ING2 were perturbed in NMR spectra of the protein during gradual addition of inositol 1,5-bisphosphate (Ins(1,5)P_2), the head group of PtdIns(5)P (Supporting Information Figures S5 and S6). Supporting Information Figure S5 shows normalized backbone amide chemical shift changes in 0.2 mM ING2 induced by 24 mM Ins(1,5)P_2, while Supporting Information Figure S6 plots chemical shift changes versus Ins(1,5)P_2 concentration from 2 to 24 mM. Thus, both of the predicted basic regions of ING2 are involved in the coordination of the inositol head group.

In conclusion, the phosphatase-resistant PtdIns(5)P analogues should provide useful tools for further in vivo research on several physiologically important pathways, including those governed by ING2. The molecular modeling presented herein provides the first model of the full ING2 C-terminus and reveals the possible binding mode of PtdIns(5)P (and its analogues) with ING2. These interactions support the biological results, provide new 3D structural information, and offer testable structure−activity hypotheses for further studies on the physiology of PtdIns(5)P binding proteins.

Experimental Methods

General Chemical Reagents and Methods. Chemicals were purchased from Aldrich and Acros Chemical Corp. and used without prior purification. Solvents were reagent-grade and distilled before use: CH_2Cl_2 was distilled from CaH_2, and THF was distilled from sodium wire. TLC used precoated silica gel aluminum sheets (EM Science silica gel 60F_{254}). Flash chromatography (FC) employed Whatman 230∼400 mesh ASTM silica gel. NMR spectra were recorded on a Varian INOVA 400 at 400 MHz (^{1}H), 101 MHz (^{13}C), 162 MHz (^{31}P), and 376 MHz (^{19}F) at 25 °C. Chemical shifts are reported in ppm with TMS as internal standard (= 0.00); ^{31}P, 85% H_3PO_4 (= 0.00); ^{19}F, $CFCl_3$ (= 0.00). Low- and high-resolution mass spectra were obtained on HP5971A MSD and Finnigan MAT95 double-focusing mass spectrometer (MS) instruments, respectively.

1D-1-*O*-(*tert*-Butyldiphenylsilyl)-2,3,4,6-*O*-tetrakis(methoxymethylene)-*myo*-inositol (7). To a solution of **6** (440 mg, 0.63 mmol) in methanol (5 mL) was added sodium methoxide (4 mL, 25% solution in anhydrous methanol). The mixture was stirred at room temperature for 24 h, then 10 mL of ethyl acetate was added, and the mixture was stirred for 20 min. The organic layer was washed with water and dried over anhydrous sodium sulfate. After filtration and concentration, the subsequent chromatography on silica gel (acetone/hexanes, 1:3) afforded **7** (330 mg, 88%) as a pale yellow oil. ^{1}H NMR (400 MHz, $CDCl_3$) 7.71 (m, 4H), 7.41 (m, 6H), 4.78 (m, 2H), 4.74 (d, J = 6.0 Hz, 1H), 4.67 (d, J = 6.0 Hz, 1H), 4.62 (d, J = 6.0 Hz, 1H), 4.52 (d, J = 6.0 Hz, 1H), 4.42 (d, J = 6.0 Hz, 1H), 4.39 (d, J = 6.0 Hz, 1H), 3.77 (m, 3H), 3.57 (m, 1H), 3.42 (s, 3H), 3.35 (s, 3H), 3.31 (s, 3H), 3.26 (m, 2H), 3.23 (s, 3H), 1.07 (m, 9H). MALDI-HRMS [M + Na]$^+$ calcd for $C_{30}H_{46}O_{10}SiNa$, 617.2752; found, 617.2749.

1D-1-*O*-(*tert*-Butyldiphenylsilyl)-5-(dimethyl methylenephosphonate)-2,3,4,6-*O*-tetrakis(methoxymethylene)-*myo*-inositol (8). To a solution of **7** (115 mg, 0.19 mmol) in THF (10 mL) was added NaH (100 mg) at 0 °C, and the mixture was stirred for 20 min. Then, dimethylphosphonomethyltriflate was added, and the mixture was warmed to room temperature and stirred for 12 h. Ethyl acetate was added, and the organic layer was washed with water, dried over anhydrous sodium sulfate, concentrated, and chromatographed on silica gel (acetone/hexanes, 1:1) giving product **8** (120 mg, 86%) as a colorless oil. ^{1}H NMR (400 MHz, $CDCl_3$) 7.70 (m, 4H), 7.41 (m, 6H), 5.02 (d, J = 6.4 Hz, 1H), 4.81 (m, 3H), 4.55 (d, J = 6.4 Hz, 1H), 4.46 (d, J = 6.4 Hz, 1H), 4.39 (d, J = 6.4 Hz, 1H), 4.29 (m, 1H), 4.18−4.12 (m, 2H), 4.01 (t, J = 9.6 Hz, 1H), 3.85−3.74 (m, 8H), 3.49 (s, 3H), 3.38 (s, 3H), 3.24 (s, 3H), 3.20 (s, 1H), 3.12 (s, 3H), 3.08 (m, 2H), 1.09 (s, 9H); ^{13}C NMR (101 MHz, $CDCl_3$) 136.3, 136.1, 134.3, 133.0, 130.3, 130.0, 128.1, 127.9, 99.2, 98.6, 97.4, 95.2, 85.6, 85.5, 79.0, 77.8, 75.6, 75.8, 74.1, 67.4, 65.8, 57.0, 56.6, 55.8, 55.6, 53.1, 53.0, 27.4, 19.3; ^{31}P NMR (162 MHz, $CDCl_3$) 24.7. MALDI-HRMS [M + Na]$^+$ calcd for $C_{33}H_{53}O_{13}SiPNa$, 739.2885; found, 739.2888.

1D-5-(dimethyl methylenephosphonate)-2,3,4,6-*O*-tetrakis(methoxymethylene)-*myo*-inositol (9). To a solution of **8** (125 mg, 0.17 mmol) in THF (5 mL) was added TBAF·$3H_2O$ (150 mg). Then, the mixture was stirred at room temperature for 4 h. The solvent was evaporated off, and the residue was chromatographed on silica gel (acetone/hexanes, 2:1) giving product **9** (80 mg, 96%) as a colorless oil. ^{1}H NMR (400 MHz, $CDCl_3$) 4.83−4.69 (m, 8H), 4.16 (d, J = 10.0 Hz, 2H), 4.05 (m, 1H), 3.91 (t, J = 9.2 Hz, 1H), 3.79 (d, J = 10.4 Hz, 6H), 3.70 (t, J = 9.2 Hz, 1H), 3.38−3.27 (m, 14H), 3.18 (t, J = 9.2 Hz, 1H); ^{13}C NMR (101 MHz, $CDCl_3$) 98.8, 98.6, 98.2, 96.4, 85.7, 85.5, 83.3, 77.8, 77.6, 76.3, 71.0, 67.7, 66.0, 56.6, 56.3, 55.9, 53.1 (m); ^{31}P NMR (162 MHz, $CDCl_3$) 24.4. MALDI-HRMS $[M + Na]^+$ calcd for $C_{17}H_{35}O_{13}PNa$, 501.1708; found, 501.1712.

1D-*O*-(1,2-Di-*O*-butanoyl-*sn*-(2S)-glycerol-3-*O*-(cyanoethyl)phospho)-5-(dimethyl methylenephosphonate)-2,3,4,6-*O*-tetrakis(methoxymethylene)-*myo*-inositol (11a). To a solution of **9** (40 mg, 0.084 mmol) in dichloromethane (2 mL) was added 1*H*-tetrazole (20 mg) and *N*,*N*-diisopropyl-*O*-(cyanoethyl)-*O*-(dibutanoyl-*sn*-(2S)-glycerol)-phosphonamidite (**10a**, 100 mg) at room temperature under Ar. After stirring the mixture at room temperature for 24 h, *t*-BuOOH (0.1 mL) was added for oxidation, and the mixture was stirred for 1 h. The solution was diluted by CH_2Cl_2 (20 mL) and washed with 10% sodium bisulfite, then dried over anhydrous sodium sulfate. After filtration and concentration, the residue was chromatographed on silica gel (acetone/hexanes, 2:1 then 3:1) giving product **11a** (45 mg, 65%) as a colorless oil. ^{1}H NMR (400 MHz, $CDCl_3$) 5.17 (m, 1H), 4.74−4.58 (m, 8H), 4.26−4.02 (m, 10H), 3.89−3.80 (m, 2H), 3.70 (d, J = 10.8 Hz, 6H), 3.39−3.27 (m, 13H), 3.07 (t, J = 9.2 Hz, 1H), 2.67 (m, 2H), 2.20 (m, 4H), 1.52 (m, 4 H), 0.83 (m, 6H); ^{13}C NMR (101 MHz, $CDCl_3$) 173.2, 172.8, 116.7, 98.8, 98.7, 98.6, 97.7, 96.2, 85.5, 85.4, 77.5, 76.7, 75.6, 75.5, 74.7, 69.4, 69.3, 67.6, 66.29, 66.28, 66.25, 66.24, 66.0, 62.56, 62.55, 62.52, 62.51, 61.6, 56.8, 56.7, 56.6, 56.0, 55.9, 53.1, 53.0, 36.1, 35.9, 19.8, 19.7, 18.4, 13.7, 13.6; ^{31}P NMR (162 MHz, $CDCl_3$) 23.9, −1.09, −1.15. MALDI-HRMS $[M + Na]^+$ calcd for $C_{31}H_{57}O_{20}NP_2Na$, 848.2841; found, 848.2849.

1D-*O*-(1,2-Di-*O*-oleoyl-*sn*-(2S)-glycerol-3-*O*-(cyanoethyl)phospho)-5-(dimethyl methylenephosphonate)-2,3,4,6-*O*-tetrakis(methoxymethylene)-*myo*-inositol (11b) was obtained from **9** and **10b** as described for **11a**, yield 45%. ^{1}H NMR (400 MHz, $CDCl_3$) 5.32 (m, 4H), 5.25 (m, 1H), 4.84−4.67 (m, 8H), 4.35−4.08 (m, 10H), 3.98−3.90 (m, 2H), 3.70 (dd, J = 2.8, 10.8 Hz, 6H), 3.49 (d, J = 10.0 Hz, 1H), 3.44 (s, 3H), 3.43 (s, 3H), 3.39 (s, 3H), 3.37 (s, 3H), 3.17 (dt, J = 2.8, 9.2 Hz, 1H), 2.76 (m, 2H), 2.31 (m, 4H), 1.98 (m, 8H), 1.58 (m, 4H), 1.28 (m, 40H), 0.85 (m, 6H); ^{13}C NMR (101 MHz, $CDCl_3$) 173.4, 173.0, 130.2, 129.9, 116.6, 98.9, 98.8, 98.7, 97.7, 96.2, 96.1, 85.5, 85.4, 77.2, 76.7, 75.6, 75.5, 74.7, 69.4, 69.3, 67.8, 66.3, 66.2, 66.1, 62.5, 62.4, 61.7, 56.9, 56.8, 56.7 56.1, 55.9, 55.8, 53.1, 53.0, 34.2, 34.1, 31.7, 29.97, 29.94, 29.73, 29.53, 29.45, 29.42, 29.35, 29.32, 29.29, 27.4, 25.0, 22.9, 19.8, 19.7, 14.3; ^{31}P NMR (162 MHz, $CDCl_3$) 24.0, −0.97, −0.99. MALDI-HRMS $[M + Na]^+$ calcd for $C_{59}H_{109}O_{20}NP_2Na$, 1236.6910; found, 1236.6934.

1D-*O*-(1,2-Di-*O*-butanoyl-*sn*-(2S)-glycerol-3-phospho)-5-(methylenephosphonate)-*myo*-inositol (1). To a solution of **11a** (18 mg, 0.021 mmol) in MeCN (1 mL) was added triethylamine (0.5 mL) and bis-(trimethylsilyl)trifluoroacetamide (BSTFA, 0.5 mL) at room temperature under Ar. After stirring the mixture at room temperature for 24 h, the solvent was removed completely in vacuum. The residue was dissolved in CH_2Cl_2 (1 mL), added to trimethylsilyl bromide (TMSBr, 0.5 mL) and BSTFA (0.5 mL), then stirred at room temperature under Ar for 10 h. After concentration, methanol (1 mL) was added, and the mixture was stirred for 1 h. The solution was evaporated and treated with cation-exchange resin (Dowex 50W-X8, 400 mesh) to give **1** (9 mg, 75%). ^{1}H NMR (400 MHz, CD_3OD) 5.24 (m, 1H), 4.36 (m, 1H), 4.26 (m, 1H), 4.14 (m, 3H), 3.99 (m, 1H), 3.80 (m, 3H), 3.66 (m, 1H), 3.39 (t, J = 9.2 Hz, 1H), 3.15 (t, J = 9.2 Hz, 1H), 2.28 (dd, J = 7.6, 16.0 Hz, 4H), 1.58 (p, J = 6.8 Hz, 4H), 0.89 (q, J = 6.8 Hz, 6H); ^{13}C NMR (101 MHz, D_2O) 173.3, 172.9, 85.4, 85.3, 81.2, 77.9, 75.0, 74.6, 71.9, 71.6, 70.2, 68.2, 67.7, 66.3, 62.4, 61.5, 35.7, 35.6, 18.1, 12.9, 12.8; ^{31}P NMR (162 MHz, D_2O) 19.3, 0.73 (m). MALDI-HRMS $[M]^+$ calcd for $C_{18}H_{34}O_{16}P_2$, 568.1322; found, 568.1299.

1D-*O*-(1,2-Di-*O*-oleoyl-*sn*-(2S)-glycerol-3-phospho)-5-(methylenephosphonate)-*myo*-inositol (2) was obtained from **11b** as described for **1**, yield 70%. ^{1}H NMR (400 MHz, $CD_3OD-CDCl_3$) 5.31 (m, 5H), 4.19−4.07 (m, 5H), 4.00 (m, 2H), 3.93 (t, J = 9.2 Hz, 1H), 3.74 (m, 2H), 3.39 (m, 1H), 3.11 (t, J = 9.2 Hz, 1H), 2.23 (m, 4H), 2.01 (m, 8H), 1.56 (m, 4H), 1.13 (m, 40H), 0.87 (t, J = 6.8 Hz, 6H); ^{13}C NMR (101 MHz, $CD_3OD-CDCl_3$) 173.2, 172.7, 129.7, 129.6, 85.9, 78.1, 77.7, 75.5, 74.9, 72.5, 72.3, 71.5, 71.3, 69.5, 68.6, 66.4, 62.5, 61.9, 33.8, 33.7, 31.8, 29.68, 29.60, 29.45, 29.30, 29.23, 29.19, 29.12, 29.09, 29.02, 27.0, 24.8, 22.6, 13.5, 13.4; ^{31}P NMR (162 MHz, $CD_3OD-CDCl_3$) 21.2, 0.68 (m). MALDI-HRMS $[M - H]^-$ calcd for $C_{46}H_{85}O_{16}P_2$, 955.5318; found, 955.5345.

1D-1-*O*-(*tert*-Butyldiphenylsilyl)-5-(bis(cyanoethyl)phosphothionate)-2,3,4,6-*O*-tetrakis(methoxymethylene)-*myo*-inositol (12). To a solution of **7** (100 mg, 0.17 mmol) in acetonitrile (5 mL) was added 1*H*-tetrazole (3% in MeCN, 0.09 mL, 0.39 mmol) and bis(2-cyanoethyl)-diisopropylphosphorodiamidite (50 mg, 0.185 mmol) at room temperature under Ar, and the mixture was stirred for 2 h. Then, sulfur (180 mg) and CS_2/Py (1:1, 1.8 mL) were added, and the mixture was stirred at room temperature for 3 h. After filtration, the filtrate was concentrated and chromatographed on silica gel (acetone/hexanes, 1:3) giving product **12** (100 mg, 75%) as a colorless oil. ^{1}H NMR (400 MHz, $CDCl_3$) 7.70 (m, 4H), 7.41 (m, 6H), 4.94 (d, J = 6.0 Hz, 1H), 4.88 (d, J = 6.0 Hz, 1H), 4.74 (m, 2H), 4.57 (d, J = 6.4 Hz, 1H), 4.48 (d, J = 6.0 Hz, 1H), 4.39−4.29 (m, 6H), 4.18 (d, J = 7.2 Hz, 1H), 4.07 (m, 1H), 3.82 (m, 2H), 3.49 (s, 3H), 3.37 (s, 3H), 3.25 (s, 3H), 3.22 (m, 1H), 3.15 (m, 1H), 3.10 (s, 3H), 2.76 (m, 4H), 1.09 (s, 9H); ^{13}C NMR (101 MHz, $CDCl_3$) 136.2, 136.0, 134.1, 132.7, 130.4, 130.2, 128.2, 128.0, 117.0, 99.3, 98.6, 97.5, 95.4, 80.7, 80.6, 77.3, 76.6, 75.4, 75.2, 74.1, 62.84, 62.83, 62.78, 62.77, 57.3, 57.0, 55.9, 55.7, 27.5, 19.5, 19.4, 19.3; ^{31}P NMR (162 MHz, $CDCl_3$) 69.1. MALDI-HRMS $[M + Na]^+$ calcd for $C_{36}H_{53}N_2O_{12}SSiPNa$, 819.2718; found, 819.2708.

1D-5-(Bis(cyanoethyl)phosphothionate)-2,3,4,6-*O*-tetrakis-(methoxymethylene)-*myo*-inositol (13). Method A. A solution of **12** (100 mg, 0.125 mmol) in THF (5 mL) was added to hydrogen fluoride−pyridine complex (70%, 0.6 mL) at room temperature in a Teflon container. After stirring for 3 weeks, the solution was diluted with ethyl acetate and washed with 10% Na_2CO_3. The organic layer was collected and dried over anhydrous sodium sulfate. After filtration, the filtrate was concentrated and chromatographed on silica gel (acetone/hexanes, 1:2) giving product **13** (50 mg, 71%) as a colorless oil.

Method B. To a solution of **16** (20 mg, 0.030 mmol) in methanol (0.5 mL) was added ammonium fluoride (20 mg), and the mixture was stirred at room temperature for 20 h. After removal of the solvent, the residue was chromatographed on silica gel (acetone/hexanes, 1:2) to afford product **13** (15 mg, 90%). ^{1}H NMR (400 MHz, $CDCl_3$) 4.82−4.68 (m, 8H), 4.22−4.12 (m, 5H), 4.05 (s, 1H), 3.94 (d, J = 7.2 Hz, 1H), 3.69 (d, J = 7.2 Hz, 1H), 3.49−3.34 (m, 14H), 2.72 (m, 4H); ^{13}C NMR (101 MHz, $CDCl_3$) 116.9, 98.8, 98.7, 98.1, 96.5, 82.2, 81.3, 76.8, 76.7, 76.3, 70.7, 62.85, 62.84, 62.77, 62.76, 57.0, 56.4, 56.0, 55.9, 19.6, 19.5; ^{31}P NMR (162 MHz, $CDCl_3$) 69.3. MALDI-HRMS $[M + Na]^+$ calcd for $C_{20}H_{35}N_2O_{12}SPNa$, 581.1541; found, 581.1526.

1D-1-*O*-(Triethylsilyl)-5-*O*-benzoxyl-2,3,4,6-*O*-tetrakis(methoxymethylene)-*myo*-inositol (14). To a solution of **6** (400 mg, 0.57 mmol) in DMF (5 mL) was added TBAF·$3H_2O$ (360 mg). The mixture was stirred at room temperature for 6 h, then diluted with 30 mL of ethyl acetate. The solution was washed with 1 N HCl, water, then dried over anhydrous sodium sulfate. After filtration and concentration, the subsequent chromatography on silica gel (acetone/hexanes, 1:5) afforded pure product (250 mg, 95%) as a colorless oil. ^{1}H NMR (400 MHz, $CDCl_3$) 8.11 (d, J = 6.8 Hz, 2H), 7.55 (t, J = 7.2 Hz, 1H), 7.43 (m, 2H), 5.27 (t, J = 9.6 Hz, 1H), 4.87 (d, J = 6.8 Hz, 1H), 4.82−4.68

(m, 5H), 4.58 (t, $J = 6.8$ Hz, 2H), 4.13 (m, 2H), 3.87 (t, $J = 9.6$ Hz, 1H), 3.69 (dd, $J = 2.4$, 9.6 Hz, 1H), 3.61 (d, $J = 9.6$ Hz, 1H), 3.46 (s, 3H), 3.39 (s, 3H), 3.25 (s, 3H), 3.02 (s, 3H); ^{13}C NMR (101 MHz, $CDCl_3$) 166.0, 133.3, 130.3, 129.9, 128.6, 98.4, 98.3, 98.1, 96.3, 81.2, 77.9, 76.9, 76.6, 74.0, 71.3, 56.2, 56.1, 56.0, 55.9. MALDI-HRMS [M + Na]$^+$ calcd for $C_{21}H_{32}O_{11}Na$, 483.1837; found, 483.1829. The obtained alcohol (150 mg, 0.33 mmol) was dissolved in CH_2Cl_2 (8 mL), then imidazol (100 mg, 1.47 mmol) and triethylsilyl chloride (0.15 mL, 0.89 mmol) were added. After the mixture was stirred at room temperature for 15 h, it was washed with water and dried over anhydrous sodium sulfate. After filtration and concentration, the residue was chromatographed on silica gel (acetone/hexanes, 1:4) giving product **14** (180 mg, 96%) as a pale yellow oil. ^{1}H NMR (400 MHz, $CDCl_3$) 8.09 (m, 2H), 7.48 (m, 1H), 7.35 (m, 2H), 5.16 (t, $J = 9.6$ Hz, 1H), 4.83 (d, $J = 7.2$ Hz, 1H), 4.74 (d, $J = 7.2$ Hz, 1H), 4.71 (d, $J = 7.2$ Hz, 1H), 4.70 (d, $J = 7.2$ Hz, 1H), 4.66 (s, 2H), 4.50 (d, $J = 7.2$ Hz, 1H), 4.44 (d, $J = 7.2$ Hz, 1H), 4.06 (t, $J = 9.6$ Hz, 1H), 3.94 (m, 2H), 3.61 (m, 2H), 3.36 (s, 3H), 3.35 (s, 3H), 2.95 (s, 3H), 2.88 (s, 3H), 0.90 (m, 9H), 0.54 (m, 6H); ^{13}C NMR (101 MHz, $CDCl_3$) 166.2, 133.1, 133.0, 130.7, 129.9, 128.5, 98.3, 98.1, 97.2, 95.9, 82.9, 80.2, 78.2, 76.9, 76.2, 73.9, 56.2, 56.1, 55.8, 55.7, 7.02, 5.04. MALDI-HRMS [M + Na]$^+$ calcd for $C_{27}H_{46}O_{11}SiNa$, 597.2702; found, 597.2704.

1D-1-*O*-(Triethylsilyl)-2,3,4,6-*O*-tetrakis(methoxymethylene)-*myo*-inositol (15). A solution of **14** (180 mg, 0.31 mmol) in CH_2Cl_2 (5 mL) was cooled to −78 °C, then added to diisobutyl aluminum hydride (1.0 M in hexane, 1.5 mL, 1.5 mmol). After the mixture was stirred at −78 °C for 2 h, methanol (3 mL) was added, and the mixture was stirred for 20 min. The residue was warmed to room temperature and poured to wet sodium sulfate. After filtration and concentration, the subsequent chromatography on silica gel (acetone/hexanes, 1:10) afforded product **15** (120 mg, 82%) as a colorless oil. ^{1}H NMR (400 MHz, $CDCl_3$) 4.84−4.70 (m, 8H), 3.94 (s, 1H), 3.81 (t, $J = 9.6$ Hz, 1H), 3.66 (t, $J = 9.6$ Hz, 1H), 3.52−3.32 (m, 15H), 0.94 (t, $J = 8.0$ Hz, 9H), 0.59 (q, $J = 8.0$ Hz, 6H); ^{13}C NMR (101 MHz, $CDCl_3$) 98.7, 98.4, 97.2, 96.0, 83.0, 80.7, 76.2, 75.4, 73.9, 72.8, 56.2, 56.1, 55.7, 55.6, 7.00, 5.05. MALDI-HRMS [M + Na]$^+$ calcd for $C_{20}H_{42}O_{10}SiNa$, 493.2445; found, 493.2316.

1D-1-*O*-(Triethylsilyl)-5-(bis(cyanoethyl) phosphothionate)-2,3,4,6-*O*-tetrakis(methoxymethylene)-*myo*-inositol (16). Bis(2-cyanethyl) diisopropyl-phosphorodiamidite (100 mg, 0.37 mmol) was added under an argon atmosphere to a solution of **15** (40 mg, 0.085 mmol) and 1*H*-tetrazole (3 wt % in MeCN, 1.2 mL, 0.52 mmol) in MeCN (2 mL). After the mixture was stirred at room temperature for 6 h, sulfur (72 mg) and CS_2/Py (1:1, 0.72 mL) were added, and the mixture was stirred for 3 h. The residue was filtered, and the filtrate was concentrated. After subsequent chromatography on silica gel (acetone/hexanes, 1:4), product **16** (45 mg, 79%) was obtained as a colorless oil. ^{1}H NMR (400 MHz, $CDCl_3$) 4.85−4.70 (m, 8H), 4.34 (m, 5H), 3.95 (m, 3H), 3.55 (dd, $J = 2.4$, 9.6 Hz, 1H), 3.48 (dd, $J = 2,4$, 9.6 Hz, 1H), 3.45 (s, 3H), 3,44 (s, 3H), 3,43 (s, 3H), 3.41 (s, 3H), 2.77 (t, $J = 6.0$ Hz, 4H), 0.97 (t, $J = 8.0$ Hz, 9H), 0.62 (q, $J = 8.0$ Hz, 6H); ^{13}C NMR (101 MHz, $CDCl_3$) 117.0, 98.7, 98.6, 97.2, 96.7, 81.0, 80.9, 76.9, 76.4, 76.2, 73.5, 62.8, 62.7, 57.1, 57.0, 56.0, 55.7, 19.5, 19.4, 7.04, 5.05; ^{31}P NMR (162 MHz, $CDCl_3$) 69.1. MALDI-HRMS [M + Na]$^+$ calcd for $C_{26}H_{49}N_2O_{12}PSSiNa$, 695.2405; found, 695.2392.

1D-1-*O*-(1,2-Di-*O*-butanoyl-*sn*-(2S)-glycerol-3-*O*-(cyanoethyl)-phospho)-5-(bis(cyanoethyl)phosphothionate)-2,3,4,6-*O*-tetrakis-(methoxymethylene)-*myo*-inositol (17a). To a solution of **13** (25 mg, 0.045 mmol) in dichloromethane (2 mL) was added 1*H*-tetrazole (20 mg) and *N*,*N*-diisopropyl-*O*-(cyanoethyl)-*O*-(dibutanoyl-*sn*-(2S)-glycerol)-phosphonamidite (**10a**, 75 mg) at room temperature under Ar. After stirring at room temperature for 24 h, *t*-BuOOH (0.1 mL) was added for oxidation, and the mixture was stirred for 1 h. The solution was diluted by CH_2Cl_2 (20 mL) and washed with 10% sodium bisulfite, then dried over anhydrous sodium sulfate. After subsequent chromatography on silica gel (acetone/hexanes, 1:1), product **17a** (20 mg, 50%) was obtained as a colorless oil. ^{1}H NMR (400 MHz, $CDCl_3$) 5.22 (m, 1H), 4.75−4.67 (m, 8H), 4.30−4.08 (m, 13H), 3.99 (t, $J = 9.6$ Hz, 1H), 3.93 (t, $J = 9.6$ Hz, 1H), 3.48 (d, $J = 9.6$ Hz, 1H), 3.39 (s, 3H), 3.37 (s, 3H), 3.34 (s, 3H), 3.33 (s, 3H), 2.72 (t, $J = 6.0$ Hz, 6H), 2.25 (m, 4H), 1.59 (m, 4H), 0.89 (m, 6H); ^{13}C NMR (101 MHz, $CDCl_3$) 173.2, 172.9, 117.0, 116.7, 98.8, 98.7, 97.8, 96.6, 80.6, 76.9, 76.1, 75.8, 74.7, 69.4, 66.3, 66.1, 63.1, 63.0, 62.7, 62.4, 61.6, 57.1, 57.0, 56.2, 55.9, 36.1, 36.0, 19.8, 19.6, 19.5, 18.4, 13.8, 13.7; ^{31}P NMR (162 MHz, $CDCl_3$) 68.99, 68.97, −1.25, −1.35. MALDI-HRMS [M + Na]$^+$ calcd for $C_{34}H_{57}O_{19}N_3P_2SNa$, 928.2674; found, 928.2717.

1D-1-*O*-(1,2-Di-*O*-oleoyl-*sn*-(2S)-glycerol-3-*O*-(cyanoethyl)phospho)-5-(bis(cyanoethyl)phosphothionate)-2,3,4,6-*O*-tetrakis(methoxymethylene)-*myo*-inositol (17b) was obtained from **13** and **10b** as described for **17a**, yield 43%. ^{1}H NMR (400 MHz, $CDCl_3$) 5.33 (m, 4H), 5.25 (m, 1H), 4.74 (m, 8H), 4.41−4.09 (m, 13H), 4.04 (t, $J = 9.6$ Hz, 1H), 3.96 (t, $J = 9.6$ Hz, 1H), 3.55 (d, $J = 9.6$ Hz, 1H), 3.43 (m, 12H), 2.77 (m, 6H), 2.32 (m, 4H), 2.00 (m, 8H), 1.59 (m, 4H), 1.28 (m, 40H), 0.87 (m, 6H); ^{13}C NMR (101 MHz, $CDCl_3$) 173.4, 173.0, 130.2, 129.9, 117.0, 116.7, 98.8, 98.7, 97.8, 96.6, 80.6, 76.1, 75.9, 75.8, 74.7, 69.5, 66.3, 66.1, 63.0, 62.6, 62.4, 61.7, 57.2, 57.0, 56.3, 56.0, 34.2, 34.1, 32.1, 29.97, 29.94, 29.73, 29.53, 29.41, 29.35, 29.30, 27.42, 27.39, 25.0, 22.9, 19.9, 19.8, 19.6, 19.5, 14.3; ^{31}P NMR (162 MHz, $CDCl_3$) 69.01, 68.99, −1.15, −1.28. MALDI-HRMS [M + Na]$^+$ calcd for $C_{62}H_{109}O_{19}N_3P_2SNa$, 1316.6743; found, 1316.6707.

1D-*O*-(1,2-Di-*O*-butanoyl-*sn*-(2S)-glycerol-3-phospho)-5-(phosphothionate)-*myo*-inositol (3). To a solution of **17a** (20 mg, 0.022 mmol) in MeCN (1 mL) was added triethylamine (0.5 mL) and bis-(trimethylsilyl)trifluoroacetamide (BSTFA, 0.5 mL) at room temperature under Ar. After stirring at room temperature for 24 h, the solvent was removed completely in vacuum. The residue was dissolved in CH_2Cl_2 (1 mL), added to trimethylsilyl bromide (TMSBr, 0.5 mL) and BSTFA (0.5 mL), then stirred at room temperature under Ar for 2 h. After concentration, methanol (1 mL) was added, and the mixture was stirred for 1 h. The solution was evaporated and treated with cation-exchange resin (Dowex 50W-X8, 400 mesh) to give **3** (8 mg, 64%). ^{1}H NMR (400 MHz, D_2O) 5.16 (m, 1H), 4.28 (dd, $J = 3.2$, 12.8 Hz, 1H), 4.10 (m, 2H), 3.94 (m, 2H), 3.83 (t, $J = 9.6$ Hz, 1H), 3.73 (t, $J = 9.6$ Hz, 1H), 3.65 (t, $J = 9.6$ Hz, 1H), 3.45 (m, 2H), 2.25 (m, 4H), 1.45 (m, 4 H), 0.75 (m, 6H); ^{13}C NMR (101 MHz, D_2O) 176.6, 176.2, 84.1, 80.1, 79.5, 76.0, 75.4, 74.1, 72.3, 71.6, 70.7, 69.5, 65.6, 63.9, 63.6, 62.8, 61.5, 35.9, 35.7, 18.1, 18.0, 12.9; ^{31}P NMR (162 MHz, D_2O) 64.7, −0.25. MALDI-HRMS [M + 3Na]$^{3+}$ calcd for $C_{17}H_{33}O_{16}P_2SNa_3$, 656.0658; found, 656.0604.

1D-*O*-(1,2-Di-*O*-oleoyl-*sn*-(2S)-glycerol-3-phospho)-5-(phosphothionate)-*myo*-inositol (4) was obtained from **17b** as described for **3**, yield 67%. ^{1}H NMR (400 MHz, CD_3OD) 5.32 (m, 5H), 4.20−3.96 (m, 3H), 3.82−3.71 (m, 3H), 3.60−3.51 (m, 2H), 3.42 (m, 2H), 2.30 (m, 4H), 2.00 (m, 8H), 1.59 (m, 4H), 1.28 (m, 40H), 0.88 (s, 6H); ^{13}C NMR (101 MHz, CD_3OD) 173.0, 172.7, 129.7, 129.6, 81.0, 79.5, 78.7, 76.9, 75.7, 75.2, 73.2, 72.1, 70.9, 68.2, 66.8, 66.2, 63.1, 61.7, 33.7, 31.8, 29.67, 29.59, 29.44, 29.28, 29.17, 29.08, 29.01, 28.97, 26.99, 26.95, 24.8, 22.5, 13.4; ^{31}P NMR (162 MHz, CD_3OD−$CDCl_3$) 63.5, 0.78 (m). MALDI-HRMS [M − H + Na]$^+$ calcd for $C_{45}H_{83}O_{15}P_2SNa$, 979.4753; found, 979.4791.

Liposome Binding Assay. The liposome binding assays were performed as described.[43] Briefly, solutions of 1-palmitoyl-2-oleoyl-*sn*-glycero-3-phosphocholine (DPPC), 1-palmitoyl-2-oleoyl-*sn*-glycero-3-phosphoethanolamine (DPPE), 1-palmitoyl-2-oleoyl-*sn*-glycero-3-phosphoserine (DPPS) (Avanti) containing either PtdIns, PtdIns(5)P, 5-MP PtdIns(5)P (**2**), 5-PT-PtdIns(5)P (**4**), or no phosphoinositide were dissolved in $CHCl_3$/MeOH/H_2O (65:25:4) and dried down under vacuum. The lipids were resuspended in 800 μL of 20 mM Tris, 100 mM KCl, pH 7.3, and sonicated using a bath sonicator for 15 min at

(43) Lee, S. A.; Eyeson, R.; Cheever, M. L.; Geng, J.; Verkhusha, V. V.; Burd, C.; Overduin, M.; Kutateladze, T. G. *Proc. Natl. Acad. Sci. U.S.A.* **2005**, *102*, 13052−13057.

25 °C. Liposomes were collected by centrifugation at 25 000*g* for 30 min and finally resuspended in 95 μL of buffer by vortexing and additional sonication for 3 min. Liposomes were incubated with 5 μL of 2 μg/μL GST−ING2 or GST for 1 h at room temperature and then collected again by centrifugation. The liposome pellets were separated from the supernatant and resuspended in 100 μL of buffer. The pellet and supernatant fractions were analyzed by SDS−PAGE using coomassie brilliant blue staining.

HT1080 Cell Death Assay. HT1080 cells were incubated with vehicle or 45 nM neocarzinostatin (Sigma), at 16 h with 10 μM of either buffer, or dipalmitoyl PtdIns, dipalmitoyl PtdIns(5)P, dioleoyl 5-MP PtdIns(5)P (**2**), or dioleolyl 5-PT-PtdIns(5)P (**4**) were added, and cells were incubated in the combined mixture for 12 additional hours. After incubation, dead cells were collected and added to the cells collected after trypsin treatment of the plates and total cells were spun down. Cell death was measured by trypan blue exclusion following the manufacturer's protocol (Invitrogen).

Molecular Modeling. The sequence of human ING2 was submitted to the SWISS-MODEL server (http://swissmodel.expasy.org/) in "first approach mode". The server provided five homologous templates in the PDB bank: 1wes, 1weu, 1wen, 2g6q, and 1x4i). Then a sequence alignment was made by the alignment module of MODELLER 8v2. On the basis of 20 models of 1x4i and 4 other templates, 20 homology models were built by MODELLER 8v2 in automodel mode. After reconstruction of the model side chains by isosterically replacing the template side chains and energy minimization by the GROMOS96 force field, the model of ING2 C-terminal was obtain as a pdb file. AutoDock3.0 software package, with the graphical user interface AutoDockTools (ADT), was used to dock small molecules (PtdIns(5)P and analogues) to the ING2 C-terminal domain. The zinc atoms in the active site were each manually assigned a charge of +2, and all other atom values were generated automatically by ADT. With the use of AutoGrid, a grid of 72 Å × 72 Å × 80 Å with 0.375 Å spacing was calculated around the docking area for the relative ligand atom types of the PtdIns(5)P and analogues. Separate docking computations were performed for each ligand using the Lamarckian genetic algorithm local search (GALS) method. The docking conformations of each ligand were clustered on the basis of root-mean-square deviation (rmsd) and ranked on the basis of free energy of binding. The top-ranked conformations were visually studied for good chemical geometry. On the basis of the complex of ING2−PtdIns(5)P, the binding interactions were determined by LIGPLOT 4.4.2 giving the hydrogen bonds and hydrophobic contacts information.

Acknowledgment. We thank the NIH (NS 29632 to G.D.P., GM 079641 to O.G., and GM 071424 and CA 113472 to T.G.K.). O.G. is a recipient of a Burroughs Wellcome CABS award and a Kimmel Scholar award. We also thank P. Neilsen (Echelon Biosciences, Inc.) for generous gifts of PtdIns(5)P and PtdIns.

Supporting Information Available: Computed docking of ligands with ING2 models; proton, carbon, and phosphorus NMR data for characterization of new compounds. This material is available free of charge via the Internet at http://pubs.acs.org.

JA070195B